REVIEW OF THE FREQUENCY STABILIZATION OF TEA CO_2 LASER OSCILLATORS

D. V. Willetts
Royal Signals and Radar Establishment
Malvern, Worcestershire
United Kingdom

SUMMARY

Most applications of TEA CO_2 lasers in heterodyne radar systems require that the transmitter has a high degree of frequency stability. This ensures good Doppler resolution and maximizes receiver sensitivity. However the environment within the device is far from benign with fast acoustic and electrical transients being present. Consequently the phenomena which govern the frequency stability of pulsed lasers are quite different from those operative in their cw counterparts. This review concentrates on the mechanisms of chirping within the output pulse; pulse to pulse frequency drift may be eliminated by frequency measurement and correction on successive pulses. It emerges that good stability hinges on correct cavity design. The energy-dependent laser-induced frequency sweep falls dramatically as mode diameter is increased. Thus it is necessary to construct resonators with good selectivity for single mode operation while having a large spot size.

INTRODUCTION

This review will attempt to explore the gradual development of the understanding of frequency chirp mechanisms in TEA CO_2 lasers from a largely historical perspective. The format of this submission will briefly review the need for frequency constancy and pertinent TEA laser technology, and then go on to examine methods of mode selection, experimental techniques and chirp mechanisms. Finally some general methods of overcoming the chirp will be described, leading on to the following paper by Harris (ref. 1) in which our favored route to alleviation of these effects so as to produce a frequency stable laser will be described.

FREQUENCY STABILITY REQUIREMENTS

Heterodyne detection results in superior sensitivity to direct detection and is in addition a fundamental requirement in Doppler velocimetry systems such as those of interest to this workshop. However, stringent frequency control is required of the transmitter laser. The theory of the required frequency characteristics of such pulsed radars has been developed by Woodward (ref. 2). He proved that range accuracy was proportional to the pulse bandwidth and Doppler accuracy to the pulse length, provided that the pulses are reproducible and that a suitable matched filter can be constructed. It should be noted that for good Doppler resolution, reproducible pulses of the required length, irrespective of frequency modulation, are adequate provided that the signal processing complexity can be tolerated. It turns out that making reproducible pulses is very difficult. There is a pulse-to-pulse energy variation in TEA laser outputs and during the course of this review it will emerge

that the frequency behavior is intimately related to output energy. Thus constructing a matched filter, not necessarily easy for nonlinear chirps, is made more complex by non-reproducibility; an active option would have to be pursued. An alternative approach is to attempt to obtain chirp-free pulses, which imposes a constraint on the laser performance while relaxing the processing requirements. In both cases an understanding of the mechanism of self frequency modulation is desired in order that the appropriate degree of frequency control may be exercised.

The accuracy of frequency measurement depends on the pulse length alone, as described above. This may be visualized as follows. N cycles of a sine wave of frequency f occupy a time T where

$$N = fT$$

The fractional frequency accuracy $\Delta f/f$ is inversely proportional to the number of cycles, the proportionality constant being about unity for SNRs of about one. Hence the frequency precision is inversely proportional to pulse length. This is a special case of the Fourier Transform limit, which states that the accuracy with which the frequency can be measured is given by the Fourier Transform of the pulse envelope. Estimates vary of the Doppler needs of a global wind sensor but the Transform-limited pulse length estimate has remained at four microseconds within a factor of two.

TEA LASERS

Discharge Technology

Figure 1 illustrates the construction of a typical small TEA laser. Two profiled electrodes of length tens of centimeters are separated by a few centimeters. The envelope contains a gas mixture of N_2, CO_2 and helium and a pulsed discharge is initiated between the electrodes by a fast switch such as a spark gap or thyratron. Discharge durations are limited to a few hundred nanoseconds by onset of the glow-arc transition; indeed, it is normally necessary to 'seed' the gas with electrons before the voltage is applied in order to obtain any glow discharge at all. For repetition rate operation of TEA lasers it is necessary to change the gas from pulse to pulse to prevent build-up of dissociation products in the active region and to replace heated gas with cool. Gas flow is usually arranged to be transverse to the optical axis but longitudinal flow devices have also been constructed. The flow duct also may contain a heat exchanger to control the gas temperature and CO oxidation catalyst.

Output Characteristics

Typical short TEA lasers emit a pulse of duration about 50 ns followed by a tail of length several microseconds as shown in figure 2. This pulse is called a gain switched spike (GSS) and is a manifestation of the significant depletion in gain that occurs when the exponentially increasing photon flux saturates the inverted medium. The tail arises from the slower energy transfer from molecular nitrogen to CO_2. Alternatively, if a standing wave of laser radiation is present within the cavity when the discharge is pulsed, the output is as shown in figure 3. Since photons do not now have to build up from noise, the threshold is crossed sooner and the optical pulse follows more quickly on the electrical discharge. The gain switching process is suppressed and the tail is enhanced, so that a longer pulse, of duration about one microsecond, results.

Finally, it must be pointed out that transverse discharges such as these may be operated in a non-self-sustained fashion by injecting electrons into the discharge from a gun. This is normally done through a very thin foil because the gun operates at much lower pressures than the laser. The field between the electrodes is then just a drift field, too low to allow the glow-arc transition to occur. Consequently the discharge can be run for very long periods and give long output pulses, such as shown in figure 4. Such discharges are also scalable to large volumes and result in particularly efficient excitation of CO_2. They are thus attractive from several points of view.

Mode Selection

Clearly, in order to assign an unambiguous value to Doppler shifts, the laser must oscillate on a single frequency, ie a single mode.

Single longitundinal mode (SLM) operation can be obtained by a variety of means. The laser can be made very short so that only one of its longitudinal modes will fit under the molecular transition bandwidth, or etalons may be incoporated within the cavity, or multiple mirror cavities can be constructed. The other means of longitudinal mode selection is to ensure that when the rapid discharge circuit is pulsed there is already within the cavity a standing field of the appropriate frequency so that one particular mode is favored over all others. One method of doing this, called hybridization, has already been alluded to, in which a CW gain section is incorporated within the pulsed cavity. The other method is to inject or seed the cavity with radiation from an external source, and this is usually called injection mode selection. It is also necessary to ensure that a single transverse mode oscillates and frequently this is done by incorporation of apertures in the cavity so as to favor the fundamental mode over higher order modes due to loss considerations. It will emerge that one means of frequency stabilization requires very large diameter modes and restrictive apertures are not suitable to the task in hand. Reference 1 discusses ways of proceeding under these circumstances.

EXPERIMENTAL METHODS

An obvious method of very high resolution spectroscopy suitable for studying small frequency changes is the use of an interferometer. Early studies (3) using a Fabry-Perot etalon met with little success since chirps of the order of a Megahertz in a source at 30 THz are being sought. This implies a resolution of about 10^8 which is asking a lot even of an interferometer. A much better route utilizes the heterodyne method and was done for the first time by Stiehl and Hoff (ref. 4). An example of this technique is illustrated in figure 5. The pulsed laser output is mixed with a cw local oscillator on a square law detector, which will respond at the difference between the two laser frequencies. The difference in frequency occurs in the RF and so standard RF analytic procedures can be used.

RESULTS

A typical beat signal arising from such a heterodyne experiment is shown in figure 6. The frequency actually increases from a value less than that of the local oscillator (LO), through a zero beat frequency, and through increasingly positive

values relative to the LO as time goes on. The envelope of the difference signal is a function of the pulse shape of the pulsed laser. The temporal dependence of frequency may be abstracted from such data by for instance measuring the positions of peaks or zero crossings in the waveform. Such a plot is shown in figure 7, where it is seen that a frequency change of about 20 MHz takes place in around two microseconds. The transform limit of such a pulse would be less than a Megahertz so such an output would be useless for accurate velocimetry.

Since the laser cavity is a Fabry-Perot etalon, frequency changes arise from changes in its optical length. On a timescale of a few microseconds, the cavity is mechanically rigid and so optical length changes arise from refractive index variations alone. Examination of figure 7 suggests that two processes are taking place, one giving rise to the early fall in frequency, and another to the rise during the remainder of the pulse. We will deal with these two phenomena in turn, dealing for convenience firstly with the effect in the tail of the pulse.

LASER-INDUCED MEDIUM PERTURBATION (LIMP)

One suggestion which was extant at the time of these experiments was that the upchirp in the tail, known to fit accurately to the square of time (ref. 5) might be due to non-uniform gas heating. The hydrodynamics of a non-uniformly heated gas have been treated by Longaker and Litvak (ref. 6), who showed that the density ρ was related to the rate of energy deposition/unit volume $\dot{E}$ by the equation

$$\frac{\partial^3 \rho}{\partial t^3} = (\gamma-1)\ \nabla^2\ \dot{E}$$

for short times t satisfying $\nu t/a \ll 1$. Here a is the characteristic size of the non-uniformity, and γ is the ratio of specific heats at constant pressure and constant volume respectively.

The density perturbation may be related to the change in refractive index by the Gladstone-Dale law

$$\frac{\partial n}{\partial t} = K \frac{\partial \rho}{\partial t}$$

where K is the Gladstone-Dale constant $(dn/d\rho)$.

Refractive index n and resonant frequency of a Fabry-Perot resonator are related by

$$\frac{dn}{n} = -\frac{d\nu}{\nu}$$

so that combining these equations we find

$$\Delta\nu(t) = \frac{K}{2}\ \nu(\gamma-1)\ \nabla^2 E\ t^2\ f(t)$$

with $f(t) = 1$ for a very short pulse (eg, a gain-switched spike (GSS)) and $f(t) = t/3\tau$ for a square pulse of length τ.

Thus the good fit of the pulse frequency to a parabolic time dependence which is observed for a GSS is immediately explained provided that $\nabla^2 E$ is constant during the pulse, ie all the energy is deposited at the beginning of the pulse. The question still arises as to whether such a non-zero $\nabla^2 E$ is produced by the electric discharge. By alteration of the discharge circuitry so as to deliberately destabilize the TEA discharge, or by the addition of low ionization potential seeds such as xylene and ferrocene, the discharge homogeneity was altered (ref. 7). No significant alteration in chirp rate resulted at constant output energy, implying that discharge non-uniformities are not the major contribution to $\nabla^2 E$. However, it was observed that the magnitude of the chirp depended on the laser energy, suggestive of a laser-induced medium perturbation (LIMP) (ref. 8). In regions of high laser intensity there is a rapid depopulation of the upper laser level by stimulated emission to the lower laser level, which rapidly undergoes V-T relaxation to the ground state. Thus the rate of deposition of translational energy E is a function of intensity, which in turn is a function of radial position, so that $\nabla^2 E$ is non-zero. A good fit to a parabolic time dependence of frequency requires that most of the translational energy is deposited at the beginning of the pulse, in other words that E should closely approximate a δ-function near the start of the pulse.

We proceed to calculate $\nabla^2 E$ as follows. Since, neglecting loss, each photon emitted by the laser results in the appearance of one CO_2 (10°0) molecule, which rapidly relaxes to CO_2 (00°0) by a V-T process, E will be equal to

$$\frac{E_L}{V}\left(\frac{\nu_o}{\nu}\right)$$

where E_L is the laser output energy, V is the mode volume, and $h\nu_o$ is the energy of the CO_2 (10°0) level above the ground state. We assume that the laser output is entirely TEM_{00} mode, whose Gaussian radial dependence may be expressed in cylindrical polar co-ordinates (r,θ,z) as

$$E_L = A \exp[-(r^2/\sigma^2)] \quad .$$

Thus

$$\nabla^2 E = \frac{4E_L}{\pi\sigma^4 \ell}\left(\frac{\nu_o}{\nu}\right)\left(\frac{r^2}{\sigma^2} - 1\right) \exp\left[-\left(\frac{r^2}{\sigma^2}\right)\right]$$

where ℓ is the active length of the TEA section. Since the refractive index follows $\nabla^2 E$, it would be desirable to find the resonant frequencies of a cavity partially filled with the appropriate non-uniform index. This difficult problem was avoided by adopting the major approximation of the analysis, namely that the index is constant at the axial value. This recognizes that most of the light is concentrated near the optical axis. The final chirp formula then becomes

$$\Delta\nu(t) = \frac{2K\nu_o(\gamma-1)\ E_L}{\pi\sigma^4\ nL}\ t^2\ f(t)$$

for a total cavity length L.

This equation summarizes the LIMP chirp completely. A linear dependence on laser output energy (power for long pulses) arises together with an inverse cavity length factor. It is noteworthy that cavity filling factor ℓ/L does not appear in

the final equation. Most importantly, however, the σ^{-4} term is the key to low chirp operation of high energy compact lasers. Accordingly experiments were carried out to test this prediction of the σ dependence (ref. 9). A plane-plane resonator configuration was chosen since σ could then readily be controlled by alteration of an intracavity aperture diameter; values between 4.2 and 8.5 mm were used. In figure 8 the normalized chirp rate is plotted against spot size σ on a log-log scale (to test a power-law dependence). It is clear that the experimental points lie close to the predicted slope of -4. However, the intercept is about one order of magnitude lower than the theoretical prediction, presumably due to the approximate modal analysis. It would appear therefore confirmed that large mode radius resonators would alleviate LIMP effects and this technique will be explored in more detail in reference 1.

Finally, the temporal dependence of chirp for long pulses was explored (ref. 10) using an e-beam sustained system whose output pulse is shown in Figure 4. Figure 9 reveals that the time dependence fits very well to the t^3 prediction rather than t^2, and figure 10 illustrates for two pulse lengths the linear dependence of chirp rate on output power. It would thus seem that a reasonable understanding of the LIMP chirp has been built up with all the parametric dependencies investigated. We now return to examine the effect at the beginning of the pulse.

PLASMA

It is clear from Figure 7 that there is a small downsweep in frequency at the start of the optical emission. The phenomenon was investigated by omission of CO_2 from the TEA laser mixture to avoid lasing and LIMP, but otherwise the arrangement of figure 5 was used. The resulting chirp on short timescales is shown in figure 11; it mirrors the shape of the current pulse very closely implying that something present during the discharge is responsible. This species must be free electrons since the contribution to the index change is <u>negative</u>. The magnitude of the process is given by the plasma dispersion function

$$\Delta n = -\omega_p^2/2\omega^2$$

where the plasma frequency ω_p is given by

$$\omega_p^2 = \frac{4\pi N e^2}{m}$$

where N is the electron density. Then it is found that

$$\Delta\nu = \frac{e^2 \ell}{2\pi m \nu L n} N$$

that is, the initial chirp should depend linearly on the electron density N. The electron density is related to the current density J by the relation

$$J = Ne\nu'$$

where ν' is the drift velocity of electrons in the gas mixture under the applied field. Thus the plasma-induced chirp should linearly follow the discharge current pulse, as observed. The measured and calculated frequency changes are in very good agreement. The process exhibited by the TEA laser pulse in figure 7 is the decay of

free electrons in the discharge tail taking place as the optical output begins. By operating the cw section of the hybrid laser below threshold, the pulse advance described earlier is reduced and optical output occurs after the electron density has decayed substantially to zero. This is shown in figure 12.

An excellent means of elimination of the plasma effect is to maintain the discharge current constant throughout the optical output pulse. This can be achieved with an e-beam sustained laser as described previously, which also possesses other desirable features for long pulse operation. However methods do exist (albeit having some drawbacks) for correcting any chirping phenomena that may be taking place, and these will now be described.

GENERAL CORRECTION TECHNIQUES

Electro-Optic Index Compensation

An obvious method to correct chirps consists of incorporating an electro-optic crystal within the laser cavity and applying a voltage to exactly compensate for any chirp process going on (ref. 11). This technique requires that the index perturbation is reproducible and is expected to be severely limited in power handling capability by optical damage to the modulator or its antireflection coatings.

Phase Conjugation

Phase conjugate mirrors have the property of reversing the wavefront incident upon them, so that a distortion caused by traverse of an index perturbed medium is removed on phase conjugate reflection through that medium. Thus a laser containing a one phase conjugate mirror can remove index perturbations within the cavity, and since frequency is simply the time derivative of phase, frequency distortions will also be removed. Figure 13 shows the apparatus used by Ouhayoun (ref. 12) to obtain phase conjugation by degenerate four-wave mixing (DFWM) in saturated CO_2. Pump radiation is provided by a loosely focused cw laser and its reflection in the cavity hard mirror; the pulsed laser output should lock in frequency to the cw laser. Current experiments have not established unambiguously that frequency locking is taking place due to the finite pulse length and the use of a Fourier Transform method of frequency examination. Assuming that frequency locking does occur, these systems do suffer from the inefficiency consequent upon using the phase conjugate approach.

Slow Vibration-to-translation* Transfer

It was stated earlier that translational heating of the ground state from the lower laser level is very fast; in fact the process typically takes a few hundred nanoseconds at atmospheric pressure. If this V-T transfer can be forced to occur on a timescale larger than the optical pulse, insignificant chirping due to LIMP will occur. The transfer can be slowed by manipulation of the gas composition or reduction of the gas pressure. Figure 14 compares the frequency sweeping for infinitely fast V-T transfer with a finite transfer rate of T^{-1}. For long times the two curves are displaced by T in time and T^2 in frequency. For short times, the region of main

*Vibration-to-translation (V-T).

interest, as much as an order of magnitude chirp reduction can result, but at the cost of reduced pressure and thus an output energy reduction.

CONCLUSIONS

The foregoing review attempts to show that the chirping mechanisms in pulse CO_2 lasers are now well understood. In particular it should be noted that these mechanisms are independent of details such as method of longitudinal mode selection and apply to all TEA CO_2 lasers. Two phenomena are of importance: a plasma effect at the beginning of the pulse and a laser induced effect during the remainder of the pulse. The latter is dependent on the laser output energy and especially on the intracavity beam size. Since these phenomena are well understood it is possible to alleviate the chirping effects by appropriate measures, of which the most practical is correct resonator design. This subject will be examined in detail in the next paper.

REFERENCES

1 Harris, M. R.: Large Mode Radius Resonators. NASA/RSRE Workshop on Closed-Cycle, Frequency-Stable CO_2 Laser Technology. NASA CP-2456, 1987.

2 Woodward, P. M.: Probability and Information Theory with Applications to Radar. Pergamon Press, 1953.

3 Nurmikko, A., Detemple, T., and Schwarz, S.: Appl. Phys. Letts. 18, 130 (1971).

4 Stiehl, W. A. and Hoff, P. W.: Appl. Phys. Letts. 22, 680 (1973).

5 Pace, P. and Lacombe, M.: Can. J. Phys. 57, 1350 (1979).

6 Longaker, P. R. and Litvak, M. M.: J. Appl. Phys. 40, 4033 (1969).

7 Willetts, D. V. and Harris, M. R.: J. Phys. D15, 51 (1982).

8 Roper, V. G., Lamberton, H., Parcell, E., and Manley, A., Opt. Commun. 25, 235 (1978).

9 Willetts, D. V. and Harris, M. R.: IEEE J. Quant. Electron. QE-19, 810 (1983).

10 Willetts, D. V. and Harris, M. R.: Opt. Commun. 49, 151 (1984).

11 Willetts, D. V. and Harris, M. R.: J. Phys. D18, 185 (1985).

12 Ouhayoun, M.: Proc. CLEO 85. Baltimore, M. A. (1985).

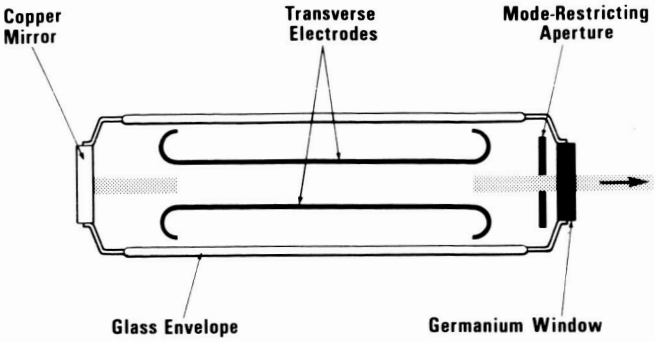

Figure 1. Longitudinal section of typical TEA CO_2 laser.

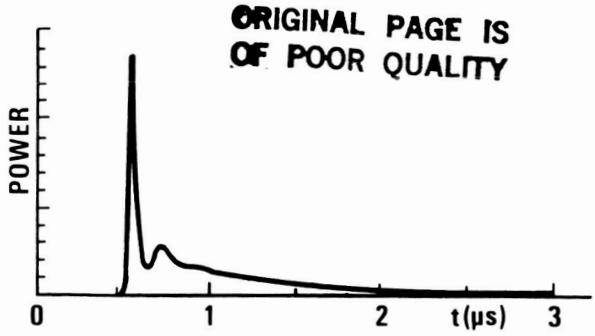

Figure 2. Output pulse shape of a simple self-sustained CO_2 TEA laser. Output energy 80 mJ.

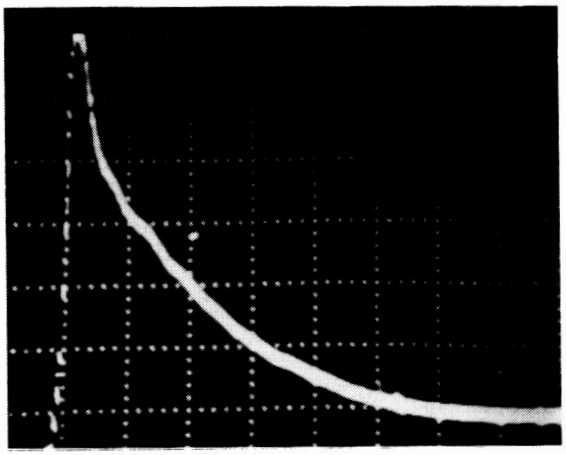

Figure 3. Output pulse shape of a hybrid self-sustained CO_2 TEA laser. Output energy 80 mJ, timescale 0.5 μs/division.

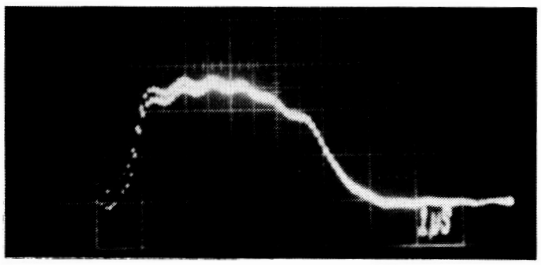

Figure 4. Output pulse shape of a hybrid electron-beam sustained CO_2 TEA laser. Output energy 80 mJ, timescale 1 μs/division.

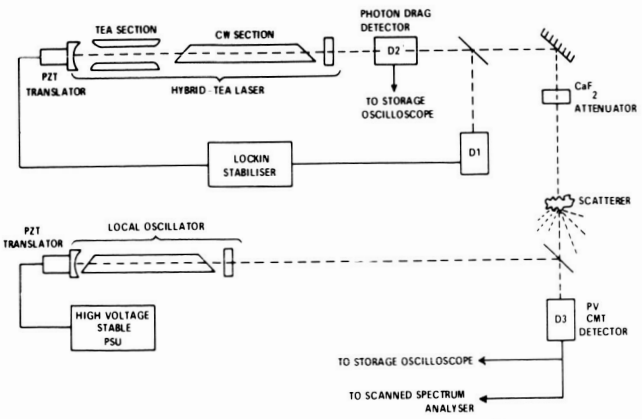

Figure 5. Typical heterodyne equipment for the determination of the frequency characteristics of a CO_2 TEA laser.

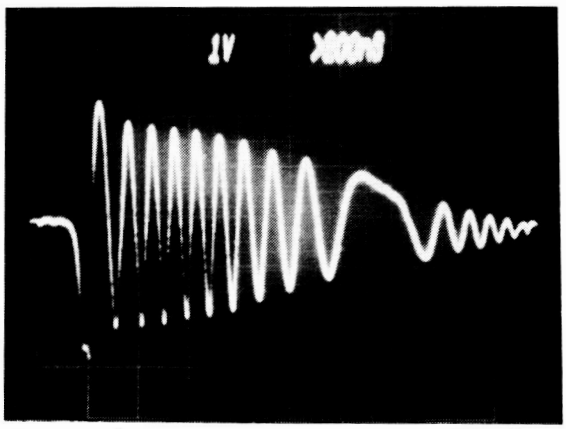

Figure 6. Example of beat signal between LO and TEA CO_2 laser. Timescale 300 ns/division.

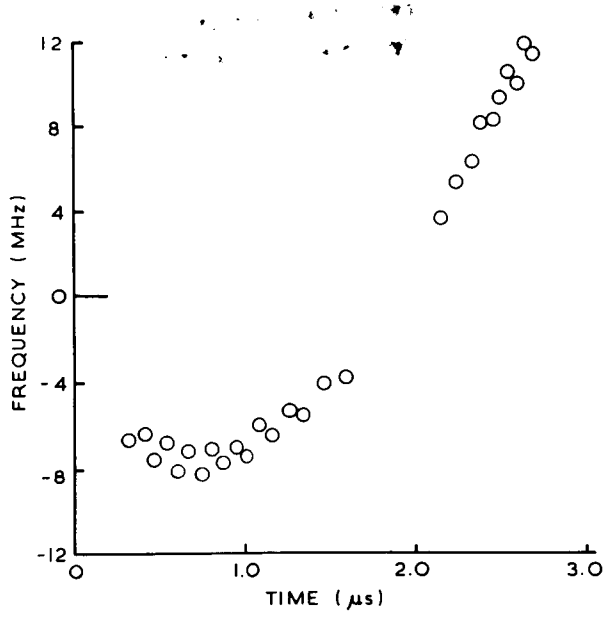

Figure 7. Frequency behavior derived from Figure 6. Frequency increases in the tail of the pulse at 3.0 MHz/μsec.

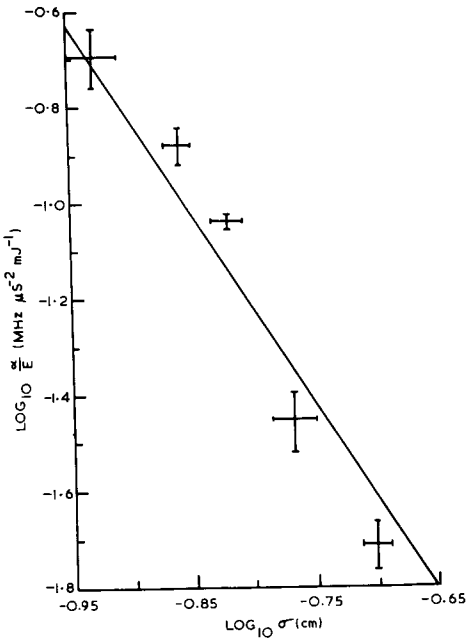

Figure 8. Chirp coefficient versus spot size for injection mode selected CO_2 laser. Line of predicted slope (-4) is shown for comparison.

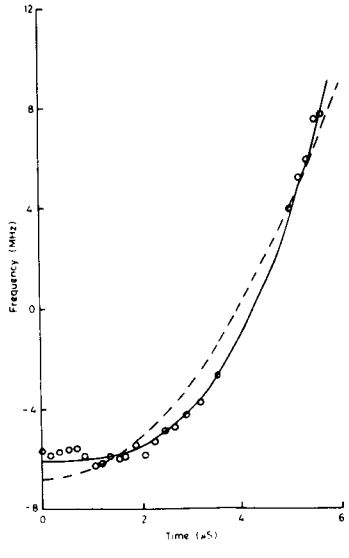

Figure 9. Frequency behavior of hybrid e-beam sustained CO_2 laser (circles). Best fit parabolic and cubic curves shown by dashed and solid lines, respectively.

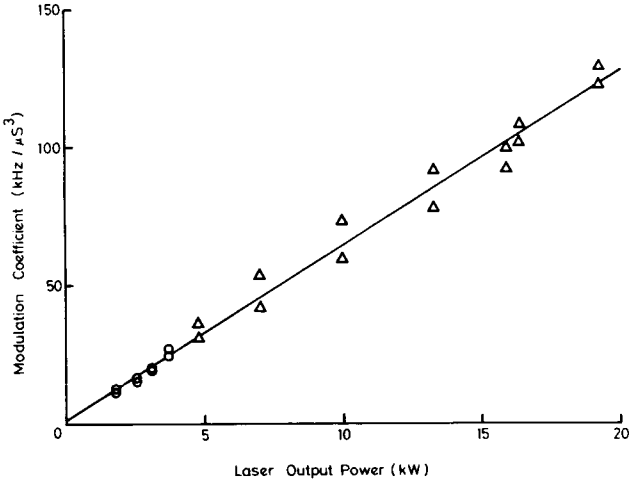

Figure 10. Graph illustrating linear dependence of modulation coefficient on output power for two different pulse lengths of an e-beam sustained TEA laser.

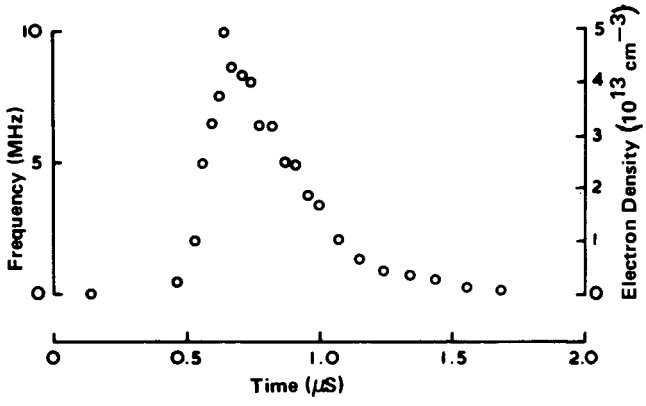

Figure 11. Plasma effect on cavity frequency during a transverse discharge.

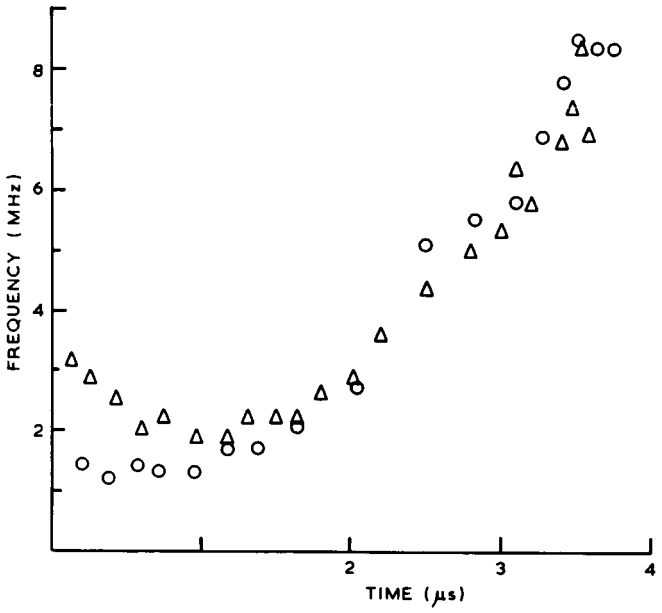

Figure 12. Frequency behavior at beginning of a hybrid laser pulse showing effect of time delay. Δ CW section above threshold, 0 CW section off.

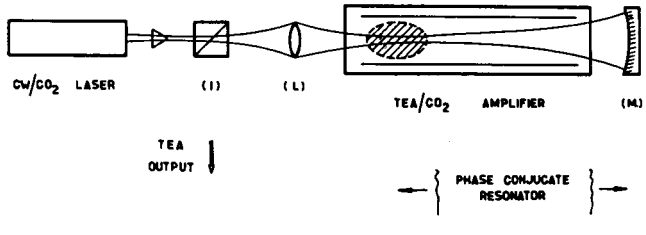

Figure 13. Frequency stabilization by phase conjugation in saturated CO_2.

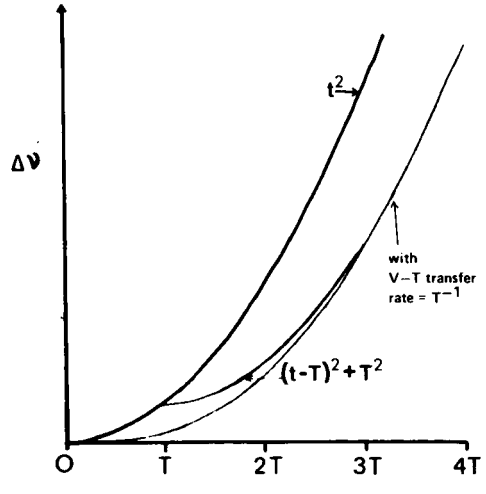

Figure 14. Effect of LIMP chirp of a finite V→T transfer rate T^{-1}.